JOC Article
pubs.acs.org/joc

Photoinduced Fluorescent Cross-Linking of 5-Chloro- and 5-Fluoro-4-thiouridines with Thymidine

Bohdan Skalski,*[,†] Katarzyna Taras-Goślińska,[†] Anna Dembska,[†] Zofia Gdaniec,[‡] and Stefan Franzen[§]

[†]*Faculty of Chemistry, Adam Mickiewicz University, Grunwaldzka 6, 60-780 Poznań, Poland,* [‡]*Institute of Bioorganic Chemistry, Polish Academy of Sciences, Z. Noskowskiego 12/14, 61-704 Poznań, Poland, and* [§]*Department of Chemistry, North Carolina State University, Raleigh, North Carolina 27695*

bskalski@amu.edu.pl

Received October 8, 2009

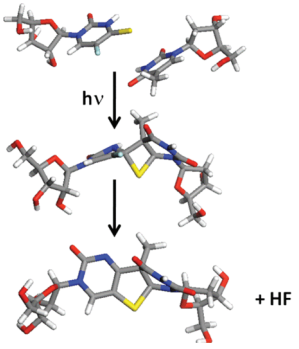

Two highly fluorescent, thermally stable diastereomeric photoadducts, **3a,b**, are formed when either 5-chloro-4-thiouridine, **1**, or 5-fluoro-4-thiouridine, **2**, are photoexcited with 366 nm UV light in the presence of thymidine (T). 5-Fluoro-4-thiouridine, **2**, exhibits photoreactivity much higher than that of the 5-chloro derivative **1**. In both cases the photoreaction is very clean, leading to highly eficient conversion of the 5-halogeno-4-thiouridine (**1**, **2**) and T to photoadducts **3a,b**. The identity and structure of **3a** was confirmed using mass spectrometry and 2-D NMR. The epimeric relationship of **3a,b** was established by UV circular dichroism spectroscopy. The geometry of the fluorescent photoadduct is consistent with formation of an interstrand cross-link in a DNA duplex if **1** or **2** is flanked by T in an opposite strand.

The 4-thiouracil (4SU) chromophore and its derivatives have attracted considerable interest in recent years as efficient photo-cross-linking agents in the studies of the structure of nucleic acids and their interactions with proteins.[1−3] The use of 4-thiouridine and 4-thiothymidine as structural probes[2,4] indicates that a range of cross-links is possible, including interstrand cross-links.[5] To identify the covalent bonds that form and to better understand the cross-linking mechanism, a number of experiments involving photoirradiation of thiouridine have been conducted in solution in the presence of common nucleosides or using dinucleotides.[6−9] In agreement with the results of 4SU photo-cross-linking experiments with DNA, it has been demonstrated that 4SU forms mixed photoadducts with all nucleobases with thymidine being the best acceptor.[8,9] The (5-4) or (6-4) bipyrimidine compounds were identified as major photoproducts of irradiation of 4SU in the presence of pyrimidine nucleosides.

(1) Favre, A. In *Bioorganic Photochemistry*; Morrison, H., Ed.; J. Wiley & Sons: New York, 1990; Vol. I, pp 379−425.
(2) Favre, A.; Saintome, C.; Fourrey, J. L.; Clivio, P.; Laugaa, P. *J. Photochem. Photobiol. B* **1998**, *42*, 109–124.
(3) Meisenheimer, K. M.; Koch, T. H. *Crit. Rev. Biochem. Mol. Biol.* **1997**, *32*, 101–140.
(4) Favre, A.; Fourrey, J. L. *Acc. Chem. Res.* **1995**, *28*, 375–382.
(5) Saintome, C.; Clivio, P.; Favre, A.; Fourrey, J. L.; Laugaa, P. *Chem. Commun.* **1997**, 167–168.
(6) Bergstrom, D. E.; Leonard, N. J. *Biochem.* **1972**, *11*, 1–9.
(7) Blazek, E. R.; Alderfer, J. L.; Tabaczynski, W. A.; Stamoudis, V. C.; Churchill, M. E.; Peak, J. G.; Peak, M. J. *Photochem. Photobiol.* **1993**, *57*, 255–265.
(8) Favre, A.; Dubreuil, Y. L.; Fourrey, J. L. *New J. Chem.* **1991**, *15*, 593–599.
(9) Peak, M. J.; Midden, W. R.; Babasick, D. M.; Haugen, D. A. *Photochem. Photobiol.* **1988**, *48*, 229–232.

DOI: 10.1021/jo902136k Published on Web 01/05/2010
© 2010 American Chemical Society

Non-native 5-halogenated pyrimidines have been studied in parallel to the 4-thiopyrimidines as probes of nucleoprotein interactions as well as DNA structure.[3]

In a search for new photoprobes, we have synthesized a series of combined 5-halogeno-4-thiouridines (5X-4SU; X = F, Cl, Br, I).[10−12] On the basis of spectroscopic and structural studies, we have recently discovered two efficiently fluorescent photoproducts that resulted from a photochemical reaction of either 5Cl-4SU (**1**) or 5F-4SU (**2**) with thymidine (T) as shown in Scheme 1. The two isomeric photoproducts **3a,b** formed in the photochemical reaction with T were the same for both **1** and **2**. Neither of these highly fluorescent photoproducts was observed for reactions of 5Br-4SU or 5I-4SU with T.

SCHEME 1. Photoreaction of 5-Halogeno-4-thiouridines 1,2 with Thymidine, T (λ_{ex} = 366 nm)

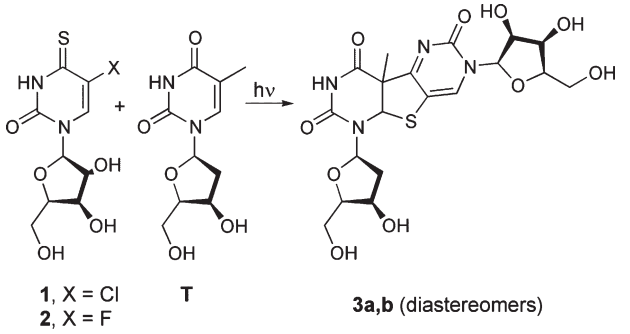

The isomeric photoproducts **3a,b** both have high fluorescence quantum yields. Moreover, our preliminary experiments indicate that analogous fluorescent adducts are formed in RNA:DNA and DNA:DNA hybrids having 5F-4SU incorporated in one of the strands, leading to highly efficient interstrand photo-cross-linking of the complementary oligonucleotides. Given the widespread use of fluorescence, the novel photoproduct we report has many potential applications. Herein, we describe the spectroscopy and structure of the two isomeric products formed when the 5-chloro-4-thiouridine or 5-fluoro-4-thiouridine are photoexcited with 366 nm light in aqueous solution in the presence of thymidine.

Figure 1 shows the changes in the absorption spectra of both **1** and T upon selective excitation of **1** at 366 nm for 75 min. The downward arrows in the figure indicate the decrease in absorption intensity of the starting materials, **1** and T, at 340 and 270 nm, respectively. The upward arrows at 242−246 nm and above 370 nm correspond to the absorption bands of the photoproducts formed. HPLC analysis of the irradiated solution reveals that both **1** and T are consumed and two photoproducts are formed. Similar spectral changes and formation of the same two photoproducts (cf. Figure 2) occur for the irradiation of **2** and T but with a ~4-fold higher rate (cf. Figure 1, Inset). This reflects much higher photoreactivity of the 5-fluoro derivative toward T and correlates well with the ratio of the measured quantum yields for the disappearance of both compounds in the presence of T (Φ = 2.8 × 10^{-3} and 6.1 × 10^{-4} for **2** and **1**, respectively).

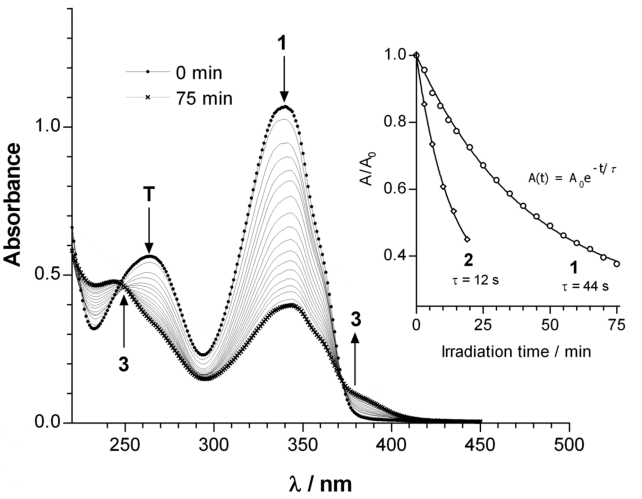

FIGURE 1. Changes in the absorption spectra of the solution of **1** and T observed during irradiation by 366 nm UV light for 75 min. The absorption band centered at 270 nm is due to T mainly, whereas that at 340 nm due to **1**. Inset: comparison of the rates of disappearance of **1** and **2** upon irradiation at 366 nm. The time constants given are 1/e times.

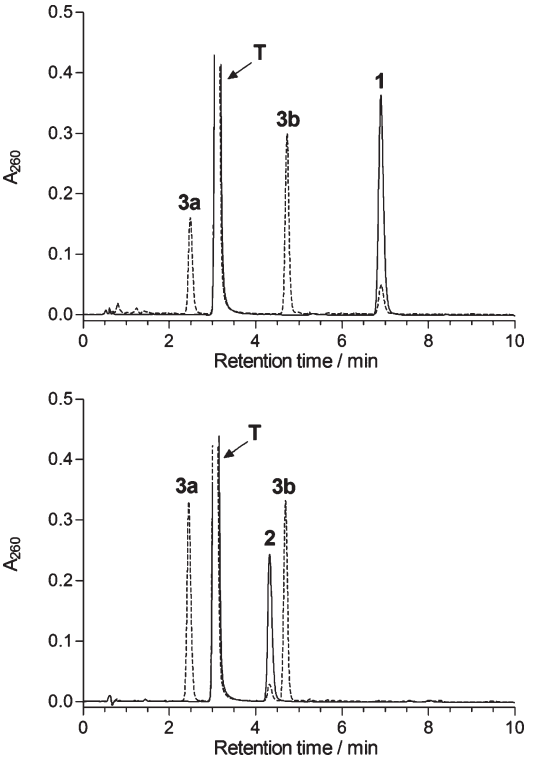

FIGURE 2. Comparison of the HPLC analyses for the preparative scale irradiations (λ_{ex} > 300 nm) of **1** (upper part) and **2** (lower part) in the presence of T (2 equiv). The solid lines correspond to the mixtures before irradiation, and dotted lines corespond to the mixtures irradiated to ca. 90% conversion of **1** and **2** (see Supporting Information for the full scale HPLC absorption and fluorescence elution profiles and respective UV spectral data). Careful analysis of the HPLC data reveals that the photoadducts **3a** and **3b** are formed with the ratios of 1:1.9 and 1:1 and overall yields of 72% and 92% for **1** and **2**, respectively.

(10) Taras-Goslinska, K.; Wenska, G.; Skalski, B.; Maciejewski, A.; Burdzinski, G.; Karolczak, J. *J. Photochem. Photobiol. A* **2004**, *168*, 227–233.
(11) Wenska, G.; Taras-Goslinska, K.; Lamparska-Kupsik, K.; Skalski, B.; Gdaniec, M.; Gdaniec, Z. *J. Chem. Soc., Perkin Trans. 1* **2002**, 53–57.
(12) Wenska, G.; Taras-Goslinska, K.; Skalski, B.; Hug, G. L.; Carmichael, I.; Marciniak, B. *J. Org. Chem.* **2005**, *70*, 982–988.

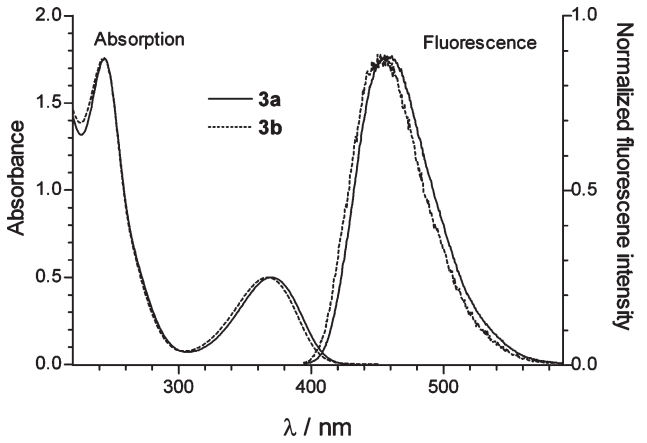

FIGURE 3. Comparison of the normalized absorption and fluorescence emission spectra of the isomers **3a** and **3b**.

TABLE 1. Measured Absorption and Fluorescence Parameters for Isomers 3a and 3b

	absorption		fluorescence		
isomer	λ_{max} (nm)	ε (M^{-1} cm^{-1})	λ_{max} (nm)	ϕ	τ (ns)
3a	244	12 800	470	0.49	14.2
	372	3 700			
3b	242	13 700	460	0.26	7.3
	367	3 800			

Figure 3 shows the normalized absorption and fluorescence spectra of the two fractions corresponding to the two photoproducts obtained from HPLC analysis. Both absorption and fluorescence spectra of species **3a** and **3b** are very similar; however, there are systematic differences as indicated in Table 1. Excitation at 360 nm produces emission at 470 nm with a quantum yield of 0.49 and 0.26 for species **3a** and **3b**, respectively. The fluorescence lifetimes of the isomers **3a** and **3b** were measured to be 14.2 and 7.3 ns, respectively. Although we do not have an explanation for the difference in quantum yield at this time, analysis of the observed lifetimes and quantum yields shows that **3a** and **3b** have nearly identical radiative lifetimes of 29 and 28 ns, respectively. Thus, the difference in their quantum yields is due to nonradiative processes, which are not included in any of the calculations presented here.

High-resolution mass spectrometry (see Supporting Information) showed that both photoproducts, **3a** and **3b**, have the same molecular composition of $C_{19}H_{24}N_4O_{10}S$, which indicates the formation of two isomers. The two isomers were formed irrespective of identity of the 5-halogen atom. The same photoaddition products were formed from the reaction of either **1** or **2** and T with a loss of HCl or HF, respectively.

The structure of both of the isomers was solved using NMR methods. The ^1H and ^{13}C NMR spectra reveal that two sugar moieties are present in the structure. The ^1H and ^{13}C signals were unambiguously assigned to ribose and deoxyribose on the basis of $^1H-^1H$ COSY and $^1H-^{13}C$ HSQC spectra (see Supporting Information). Apart from the sugar protons there are only three singlets at 8.30, 5.91, and 1.69 ppm in the ^1H NMR spectrum. These resonances had integrated intensities corresponding to 1, 1, and 3 protons, respectively. We will refer to the sugar atoms as deoxy Cn' or ribo Cn', respectively, where n represents the standard numbering.

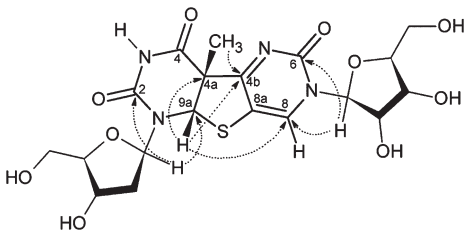

FIGURE 4. Structure of 7-(3,4-dihydroxy-5-hydroxymethyl-tetrahydro-furan-2-yl)-1-(4-hydroxy-5-hydroxy-methyl-tetrahydro-furan-2-yl)-4a-methyl-4a,9a-dihydro-1*H*,7*H*-9-thia-1,3,5,7-tetraaza-fluorene-2,4,6-trione, **3a**, confirmed by NMR spectroscopy. The arrows show the connectivity of the crosspeaks due to coupling through 2- and 3-carbon atoms observed in the HMBC experiment.

The NMR data were used to establish the identity of the photoproducts as two diastereomers. From the four theoretically possible diastereomers two would be trans-fused at the C4a−C9a bond and thus unlikely. In both the possible cis-fused diastereomers 4a-CH_3 and 9a-H are cis oriented. These two diastereomers thus form a pair of C4a,C9a-epimers. On the basis of the integration we conclude that the 1.69 ppm peak corresponds to the methyl at position C4a. Using NOEs we determined that the methyl group is cis to the 9a-H at 5.91 ppm in each of the isomers. The NOE observed between the ribo 1′-H (5.94 ppm) and the peak at 8.30 ppm permits assignment of this peak as the 8-H of the 9-thiafluorene ring. The detailed proof of the structure is presented for isomer **3a**, which is shown in Figure 4. The proof for isomer **3b** is completely analogous.

All 19 carbon signals can be identified in the ^{13}C NMR spectrum in agreement with the molecular formula. Ten ^{13}C resonances are assigned to the sugar residues (vide supra), and these are given in the Supporting Information. There are six quaternary carbon atoms, one methyl group at 17.17 ppm, and two carbon atoms at 135.88 ppm and 64.88 ppm that are directly bonded to protons at 8.30 ppm (H8) and 5.91 ppm (H9a), respectively.

The fluorene-like ring structure was established by analyzing long-range proton−carbon correlations in the $^1H-^{13}C$ HMBC spectrum. Specifically, the interconnection between two rings could be established using the correlation of carbon and hydrogen via J(CH) over two and three bonds. The proton signal at 5.94 ppm attributed to ribo H1′ correlates with signals at 155.91 ppm (C6) and 135.88 ppm (C8) in the $^1H-^{13}C$ HMBC spectrum. The deoxy H1′ exhibits a weak NOE to H9a at 5.91 ppm and shows correlations with carbon resonances at 64.88 ppm (C9a) and 152.21 ppm (C2) in the $^1H-^{13}C$ HMBC spectrum. Crosspeaks between proton H9a at 5.91 ppm and carbon atoms at 55.48 ppm (C4a), 115.38 ppm (C8a), and 174.56 ppm (C4b) establish the connectivity proposed in Figure 4. Further evidence can be in the observed correlations between the methyl protons and carbon atom at 174.56 ppm (C4b).

To further support the structure of the photoproduct, we built two models. The model with C9a-S-C8a connectivity is shown in Figure 4. A second possible model would have a C4a-S-C4b connectivity, using the numbering of the molecule in Figure 4. Analysis of these two models indicated that

only the proposed structure with C9a-S-C8a, shown in Figure 4, is possible. In the model with the C4a-S-C4b connectivity, a close contact between proton H9a and H8 would have been detected in NOE-type spectra and the strong cross peak between the methyl protons and C4b would have been absent in $^{1}H-^{13}C$ HMBC spectrum.

The epimeric relationship between **3a** and **3b** was confirmed further by their CD spectra, which are presented in Figure 5. The CD spectra indicate that the fused heterocyclic

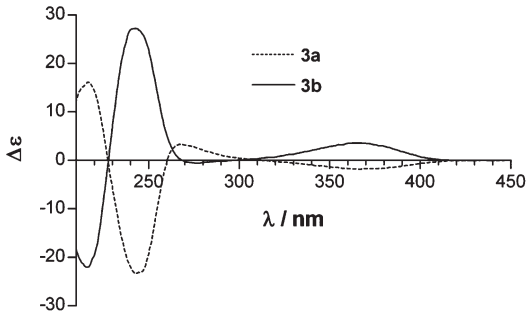

FIGURE 5. Circular dichroism spectra of isomers **3a** and **3b**.

and thus chromophoric parts of these compounds have opposite configurations, and the diastereomerism results from the presence of the two ribose residues in the structure.

The photoadducts **3a,b** are structurally distinct from a 5-4 pyrimidine-pyrimidone photoadduct formed by irradiation of 4SU in the presence of T[6,7] as well as similar 5-4 and/or 6-4 bipyrimidine products formed upon irradiation of 4SU in the presence of other pyrimidine bases.[2] Furthermore, the specificity and the overall yield of **3a** and **3b** are significantly larger than for photoadducts of 4SU with pyrimidine nucleobases. It is generally accepted that the formation of 4SU photoadducts occurs via thermally unstable thietane intermediates formed upon addition of the thiocarbonyl group of 4SU to the C5=C6 double bond of another pyrimidine. Thus, it is reasonable to assume that a similar mechanism involving the initial formation of a fluorinated or chlorinated thietane (also referred to as thietane-F and -Cl, respectively) intermediate operates also in the case of **1** and **2** (Scheme 2).

SCHEME 2. Proposed Mechanism for Formation of 3a,b

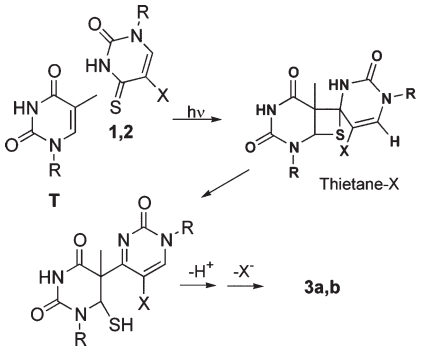

However, whereas in the case of the 4SU thietane-X intermediate (X = H) H_2S is eliminated prior the formation of a stable photoproduct, **1** and **2** undergo, when X = Cl or F, a ring opening followed by ring closure with loss of H-Cl or H-F to form the tricyclic structures of **3a** and **3b** as outlined in Scheme 2. Thus, it appears that the combination of

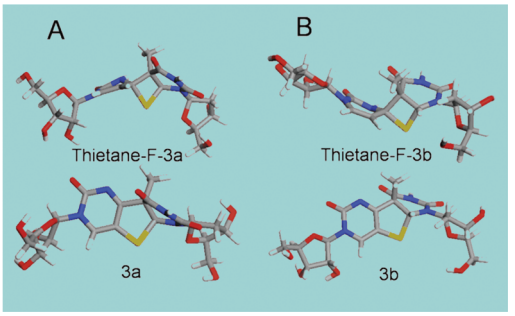

FIGURE 6. Two possible isomers obtained from calculations are indicated. (A) The thietane-F-**3a** intermediate structure is shown along with the final rearranged product, **3a**, that is formed when HF is eliminated. (B) The corresponding intermediate and final structure for isomer **3b** are shown.

C5-halogenation and C4-thionation of uridine provides both the necessary leaving group, X = F^- or Cl^-, and nucleophile, S, to promote the elimination required to form the stable tetraza fluorene product.

It was not possible to experimentally observe the thietane-X-**3a,b** intermediate that would verify the proposed mechanism; however, the mechanism is strongly supported by DFT calculations. The calculated structures of **3a,b** along with the corresponding thietane-F-**3a,b** intermediates are shown in Figure 6, whereas dissociation and rearrangement energies for the halogenated thietane-X series (X = H, F, Cl, Br, I) are presented in Figure 7.

The reactivity of the modified bases with respect to rearrangement of the thietane-X intermediate and loss of HX is in agreement with theory. Figure 7A gives the calculated bond energies of H-X (see also Supporting Information for values). The overall energies for the rearrangement of the thietane intermediate to form the fluorocrosslink product, **3a,b** is given by:

$$\text{thietane-X-}\mathbf{3a,b} \rightarrow \mathbf{3a,b} + \text{HX}$$

This reaction energy is shown in Figure 7B,C for **3a** and **3b**, respectively (see also Supporting Information). The calculations reveal that the difference in the C-X and H-X bond energies is the driving force for the rearrangement of the thietane-X-**3a,b** intermediate. Although the C−F bond is commonly regarded as the strongest bond in organic chemistry, the loss of HF can occur if there is an internal strain such as exists in the thietane-F-**3a,b** intermediate. The calculation shows that loss of H_2 is not favorable under these conditions. Both theory and experiment show that loss of HCl can also lead to formation of the fluorocrosslink product. However, as the C−X bond weakens, e.g., for C−Br and C−I, other bond breaking events can lead to other competing reactions as shown by the extensive photochemical studies of C−X bonds in the 5-halogenouridine excited states.

The fluorinated thietane intermediate has the largest driving force for rearrangement to form the photoproduct. Consequently, this molecule has the greatest yield and most favorable kinetics for formation as seen experimentally in Figure 1. The chlorinated thietane intermediate is somewhat less reactive. The brominated thietane intermediate is not predicted to rearrange to form **3a,b**, in agreement with the observation that irradiation of 5Br-4SU and T does not

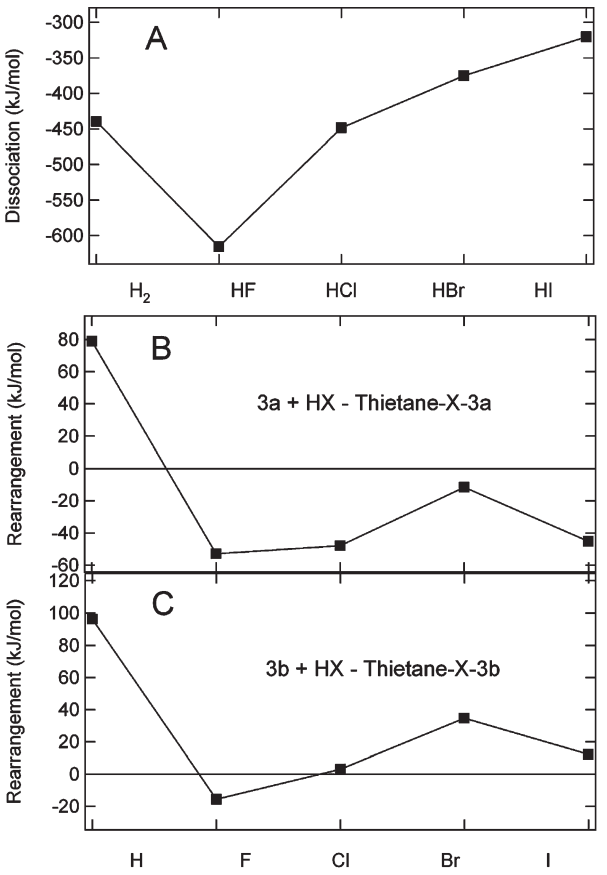

FIGURE 7. Dissociation and rearrangement energies for reactions. (A) The dissociation energies for the H-X (X = H, F, Cl, Br, I) series is presented. (B) The rearrangement energy from the thietane-X intermediate with atom X is presented for isomer **3a**. (C) The rearrangement energy is presented for isomer **3b**.

result in a fluorescent photoproduct. The case of iodine, 5I-4SU is not comparable since loss of I by photolysis is facile.[12,13] The absorption and fluorescence spectra for the model of **3a**, in which the sugar residue was replaced by a methyl group, were also calculated (Figure 8) and are in agreement with the measured spectra of **3a** shown in Figure 3.

In summary, we have studied the formation of the photoproduct of 5X-4SU and T and shown that for X = F and Cl there is a unique pair of isomeric photoproducts that form. The photoproducts are fluorophores with higher fluorescence yield than any known pyrimidine-pyrimidine adducts. The reaction does not occur for X = H, Br, or I in agreement with calculations. Thiouridine and thiothymidine have a wide range of applications including template-directed photoligation,[14] photoaffinity probes,[3,15−17] and therapeutics.[18] The 5Br-4SU

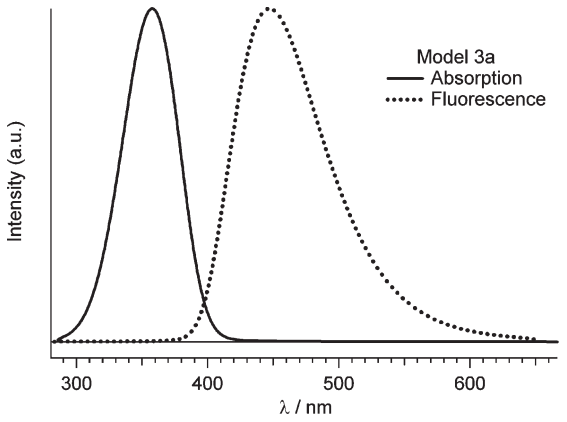

FIGURE 8. Calculated absorption and fluorescence spectra for a model of **3a**, which lacks deoxyribose and ribose sugars. The vibrational frequencies and excited state displacements were calculated using DFT methods.

has also been found to be a candidate for clinical therapeutic applications.[19] The high specificity and yield of the cross-link formed between 5F-4SU/5Cl-4SU and T presents new possibilities in each of these realms of application. The geometry formed in these solution studies is consistent with applications in DNA heteroduplexes using a 5F-4SU/5Cl-4SU modified nucleotide in an opposite flanking position to T. The creation of a fluorescent crosslink under these conditions has potential applications in both *in vitro* and *in vivo* identification of DNA sequences.

Experimental Section

Synthesis of 1 and 2. 2′,3′,5′-Tri-*O*-acetyl-5-halogeno-4-thiouridines (X = F, Cl) were prepared as previously described[11] and subjected to de-O-acetylation with 2.5% ammonium hydroxide in methanol/water mixture (1:1, v:v) to give the corresponding unprotected nucleosides **1** and **2**.

Photoreactions of 1 and 2 with T. For analytical scale experiments aqueous solutions of **1** or **2** (0.2 mmol) containing an equimolar amount of thymidine were placed in a 1 cm × 1 cm UV cell, deoxygenated by bubbling argon, and irradiated on an optical bench using a 200 W high-pressure mercury lamp equipped with an interference filter to isolate the 366 nm line. The progress of the reaction was monitored by UV spectroscopy and HPLC. The quantum yields for the disappearance of **1** and **2** were measured using benzophenone/benzhydrol actinometry.[20]

Preparative Irradiation for Product Analysis. The solutions of **1** or **2** (400 mL, 0.2 mmol) with T (2 equiv) were irradiated, in portions, in a 80 mL photoreactor with a 150 W high pressure mercury lamp through a Pyrex filter under an argon atmosphere. Irradiation was continued to ca. 95% conversion of the substrate as checked by HPLC. Irradiated solutions were collected and concentrated under reduced pressure. The photoproducts were isolated from the residue by preparative HPLC and identified by means of high resolution mass spectrometry and NMR data as discussed above.

Computational Methods. The optimized ground state geometries and potential energy surfaces Thietane-X-**1,2** and diastereomers **3a,b** were obtained using the GGA functional[21]

(13) Kawai, K.; Saito, I.; Sugiyama, H. *Tetrahedron Lett*. **1999**, *40*, 5721–5724.
(14) Liu, J. Q.; Taylor, J. S. *Nucleic Acids Res*. **1998**, *26*, 3300–3304.
(15) Podar, M.; Perlman, P. S. *RNA* **1999**, *5*, 318–329.
(16) Saintome, C.; Clivio, P.; Fourrey, J. L.; Woisard, A.; Favre, A. *Tetrahedron Lett*. **1994**, *35*, 873–876.
(17) Saintome, C.; Clivio, P.; Fourrey, J. L.; Woisard, A.; Laugaa, P.; Favre, A. *Tetrahedron* **2000**, *56*, 1197–1206.
(18) Parker, W. B.; Shaddix, S. C.; Rose, L. M.; Tiwari, K. N.; Montogmery, J. A.; Secrist, J. A. III; Bennett, L. L., Jr. *Biochem. Pharmacol*. **1995**, *50*, 687–695.
(19) Xu, Y. Z.; Zhang, X.; Wu, H. C.; Massey, A.; Karran, P. *Bioorg. Med. Chem. Lett*. **2004**, *14*, 995–997.
(20) Murov, S. L.; Carmichael, I.; Hug, G. L. *Handbook of Photochemistry*, 2nd ed.; Marcel Dekker: New York, 1993; p 307.
(21) Perdew, J. P.; Chevary, J. A.; Vosko, S. H.; Jackson, K. A.; Pederson, M. R.; Singh, D. J.; Fiolhais, C. *Phys. Rev. B* **1992**, *46*, 6671–6687.

as implemented in DMol3 (Molecular Simulations Inc.).[22] Calculations were carried at the North Carolina State University High Performance Computing Center. Geometry optimizations were carried out without constraints until the energy difference was less than 10^{-6} au on subsequent iterations. Numerically tabulated basis sets of double-ζ plus polarization (DNP) quality were employed. The difference between the minima of the ground and excited states was employed to estimate the magnitude of the nuclear displacement along each normal mode. The calculated nuclear displacements, Δ_i, provide the electron−phonon coupling constants, $S_i = \Delta_i^2/2$ for the corresponding Franck−Condon active mode of frequency ω_i, which along with temperature provides the necessary inputs for the two-time formalism. For each normal mode, the vibration displaces each respective atom constituting the structure in Cartesian space by a magnitude, Δx_i, Δy_i, and Δz_i. A dimensionless nuclear displacement, Δ, was then calculated for each displaced atom in the optimized structure. In order to verify that the modes contained a single minimum, the nuclear displacements, Q, were calculated for 11 geometries ranging from 1 au to −1 au ($Q_j = -1, -4/5, ..., 0, ..., +4/5, +1$). The displaced structure, representing the excited state for each respective mode, was found by taking the geometry optimized Cartesian coordinate for each respective atom and subtracting the mass weighted normal mode eigenvector for each respective displacement step:

$$C_j = \left(\frac{\Delta q_j}{M_w^{1/2}}\right)\left(\frac{Q_j}{0.529167}\right)$$

$q_i = x_i, y_i$, and z_i, C is the new x, y, and z coordinate, and M_w is the molecular weight of the corresponding atom. The factor of 0.529167 is the Bohr radius used to convert from atomic units to Å. The dimensionless displacements along the ith normal mode, Δ_i, was calculated by dividing the normal mode displacement by $1/\alpha_i^{1/2}$, where $\alpha_i = 2\pi\mu_i\omega_i/h$. The conversion factor $(2\pi^2 m_p c)/(10^{20}$ h) was employed to convert the energy to cm^{-1}. The time-correlator implemented in the program TIMETHERM, developed by Shreve,[23] was used to calculate absorption spectra at 300 K. The calculation also gave the Stokes shift permitting calculation of the fluorescence spectrum.

Acknowledgment. S.F. and B.S. gratefully acknowledge support from NSF grant OISE 0651876. Partial support from the Ministry of Science and Higher Education (MNiSW) Poland, project N N204 215434 is also acknowledged.

Supporting Information Available: Mass spectrometric data, NMR data, output from DFT calculations and HLPC analysis. This material is available free of charge via the Internet at http://pubs.acs.org.

(22) Delley, B. *J. Chem. Phys.* **2000**, *113*, 7756–7764.
(23) Shreve, A. P.; Mathies, R. A. *J. Phys. Chem.* **1995**, *99*, 7285–7299.